Hindawi Publishing Corporation
Journal of Nanomaterials
Volume 2016, Article ID 2840410, 10 pages
http://dx.doi.org/10.1155/2016/2840410

Research Article

Effect of Nanoparticle Surface Modification and Filling Concentration on Space Charge Characteristics in TiO_2/XLPE Nanocomposites

Youyuan Wang, Kun Xiao, Can Wang, Lijun Yang, and Feipeng Wang

State Key Laboratory of Power Transmission Equipment & System Security and New Technology, Chongqing University, Chongqing 400044, China

Correspondence should be addressed to Kun Xiao; 20104427@cqu.edu.cn

Received 14 June 2016; Revised 11 August 2016; Accepted 5 October 2016

Academic Editor: Asish Malas

This paper focuses on the space charge characteristics in TiO_2/cross-linked polyethylene (XLPE) nanocomposites; the unmodified and modified by dimethyloctylsilane (MDOS) TiO_2 nanoparticles were added to XLPE matrix with different mass concentrations (1 wt%, 3 wt%, and 5 wt%). The scanning electron microscope (SEM) showed that the MDOS coupling agent could improve the compatibility between TiO_2 nanoparticles and XLPE matrix to some extent and reduce the agglomeration of TiO_2 nanoparticles compared with unmodified TiO_2 nanoparticles; the volume resistivity testing indicated that the volume resistivity of TiO_2/XLPE nanocomposites was higher than Pure-XLPE and increased with the increase of filling concentrations. According to the pulsed electroacoustic (PEA) measurements, it was concluded that the space charge accumulation was suppressed by filling TiO_2 nanoparticles and the distribution of electric field in samples was improved greatly. In addition, it was found that the injection of homocharge was more obvious in MDOS-TiO_2/XLPE than that in UN-TiO_2/XLPE and the homocharge injection decreased with the increase of filling concentration.

1. Introduction

Cross-linked polyethylene (XLPE) has low dielectric constant, low conductivity, and stable chemical properties, which has been widely used as cable insulation material [1, 2]. However, the serious accumulation of space charge inside the XLPE has been a critical problem to be solved in the application of HVDC cable insulation, leading to distorting local electric field, accelerating insulating aging, and shortening the service life of the cable [3–5]. With the rapid development of power industry, better performance and more reliability of HVDC cable insulation material are required eagerly. Therefore, high-performance cable insulation material research has been an urgent need for engineering applications.

In recent years, the tremendous development of nanotechnology has provided a new direction for researching on properties of polymer. Domestic and foreign scholars have carried out extensive studies on the space charge characteristics of polymer nanocomposites, mainly focusing on the following aspects: (1) how the electrode materials, the thickness of samples, the aging types, and so on impact the distribution of space charge in nanocomposites [6]; (2) the space charge behaviors and inhibition mechanism of nanocomposite [7, 8]; (3) the electrical conductivity and conductance mechanism of nanocomposite [9, 10]; (4) the inhibition behaviors and inhibition mechanism of electrical and water branches in nanocomposites [11–13].

At present, the interface between nanoparticles and polymer matrix has a significant impact on the dielectric properties of the nanocomposite, which has been confirmed by domestic and foreign scholars. Several different models have been proposed to explain the specific structure and the function mechanism of interface regions. Lewis proposed an electric double layer model considering that the interface formed when the low density polyethylene (LDPE) and the nanoparticle are in contact, with LDPE being negatively charged and the nanoparticles being positively charged [14]. A "multicore model" was proposed by Tanaka et al. where they divided the interface region into three layers: bonded layer, bound layer, and loose layer, explaining well that the nanocomposite

dielectric in which the layered silicate is doped improved the performance to restrain localized discharge [15]. In Takada et al.'s paper [16], they calculated the distribution of electric field around nanoparticles under external electric field and found that the inherent dipoles such as carbonyl defects and the dipoles induced by nanoparticles will produce potential wells, thus presenting a trapping potential model to perfectly explain the space charge inhibition behavior of MgO/LDPE nanocomposite. However, these models could not fully explain the experimental results about space charge characteristics of nanocomposite, especially about the transportation behaviors of space charge, the effect of surface treatment of nanoparticles on space charge, and the relationship between space charge accumulation and nanoparticles filling concentration. In summary, more systematic and precise experiments are required to verify various existing nanocomposite theories or propose new ones, in order to eventually integrate our fragmented knowledge and understand the quantitative models. Moreover, current related researches about nanocomposites were mostly based on LDPE matrix, while the reports about XLPE matrix are very few. XLPE has been usually used as high voltage DC cable insulation material and has large difference in molecular structure compared to LDPE; thus, it is necessary to lucubrate the space charge characteristics of XLPE nanocomposite.

In this paper, the TiO_2 nanoparticles unmodified and modified by dimethyloctylsilane (DMOS) coupling agent were added to XLPE matrix with different mass concentrations (1 wt%, 3 wt%, and 5 wt%) in order to research the properties of TiO_2/XLPE nanocomposite and explain the experimental phenomenon reasonably. Scanning electron microscopy (SEM) was firstly adopted to observe the TiO_2 nanoparticle dispersion in XLPE matrix. Furthermore, the volume resistivity was carried out to analyze the movement of carriers. In addition, the pulsed electroacoustic (PEA) method was used to determine the space charge characteristics of TiO_2/XLPE nanocomposite.

2. Materials and Methods

2.1. Sample Preparation

2.1.1. Surface Modification of Nanoparticles. Common surface modification agents are shown as follows: coupling agents, surfactants, unsaturated organic acids and oligomer, organosilicon, inorganic surface treatment agents, and so on. A function of surface modification is to increase the dispersion of nanoparticle in the matrix, taking full advantage of the small dimension effect of nanoparticles, and another is to increase the compatibility between polymer matrix and nanoparticles, enhancing the interfacial chemical bond [17]. In this paper, MDOS was used as a coupling agent to modify the surface of TiO_2 nanoparticles, the chemical structure of which is shown in Figure 1.

2.1.2. TiO_2/XLPE Sample Preparation. LDPE was the master batch of XLPE, with density of 0.910~0.925 mg/cm^3, melt index of 2.1~2.2 g/10 min, and melting point of 112°C. Rutile

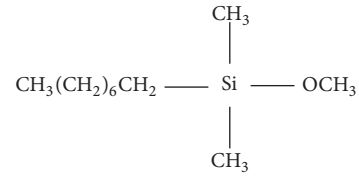

Figure 1: Chemical structure of MDOS.

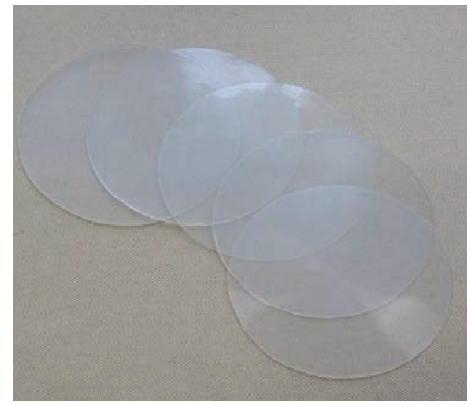

Figure 2: XLPE thin film samples.

TiO_2 nanoparticles were selected as filler, with diameter of 20~25 nm, and dicumyl peroxide (DCP) was used as a cross-linking agent. Sample preparation method is as follows: TiO_2/LDPE mixture was prepared by melting blend in an open type mixer at 115°C; the TiO_2/LDPE mixture and the DCP cross-linking agent were mixed in a closed type mixer in order to avoid pre-cross-linking at 115°C; then, the film samples with the thickness of about 170 μm were prepared by a flat vulcanizing machine at 180°C, 15 MPa, and cross-linking for 30 min; the film samples were placed in a vacuum oven in order to eliminate the residual stress and the low molecular weight byproducts during the sample preparation process, retaining 48 h at 80°C. The film samples are shown in Figure 2.

2.2. Volume Resistivity Measurement. The PC68 digital high resistance meter was used to obtain the volume resistivity. Compression moulded sheet having diameter of 100 mm was inserted into the holder and charged for more than one minute at 5000 V. The volume resistivity measurement was carried out at room temperature (25 ± 1)°C. The volume resistivity $\rho_v = A_e(R_v/d)$ Ω·m, where $A_e = 21.237$ cm^2, R_v is the volume resistance, and d is the thickness of the samples. The results are the average measurements of 5 different specimens for each sample.

2.3. Space Charge Measurement. The space charge measurement was carried out with a pulsed electroacoustic (PEA) system; the measuring principle of the device is shown in Figure 3. A narrow high voltage pulse produced by a pulse module was applied to the samples, causing the space charge in the samples to produce tiny displacement, which could be converted to electrical signal by a piezoelectric sensor. Then,

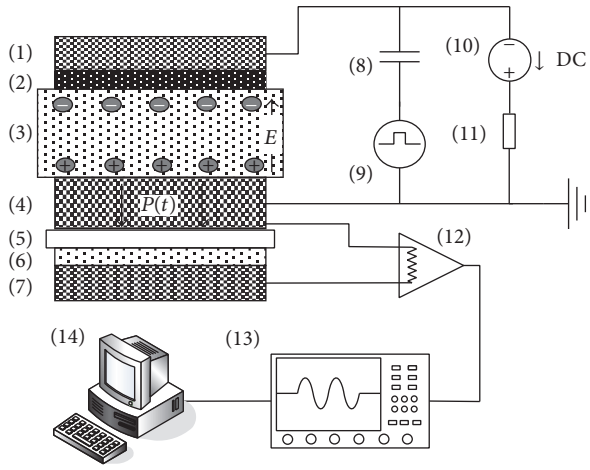

(1) Electrode (copper)
(2) Semiconductor
(3) Sample
(4) Electrode (aluminum)
(5) PVDF
(6) PMMA
(7) Electrode (aluminum)
(8) Capacitor
(9) Pulse module
(10) High voltage DC module
(11) Resistance
(12) Preamplifier
(13) Oscilloscope
(14) Computer

Figure 3: Schematic diagram of the measuring device by PEA method.

space charge distribution was collected by special software. The pulse module is produced by Canada AVTECH Company, model AVIR-1-C, pulse width 2~5 ns, pulse amplitude 200 V; the high voltage DC module is produced by Japan Matsusada Company, model AU-20R3-LC, output voltage 0~±20 kV. Silicone oil is used as an acoustic coupling agent to improve the measuring accuracy, measuring ambient temperature (25 ± 1)°C, and relative humidity (40 ± 2)%. Space charge distribution in samples under DC stress of −30 kV/mm was measured, and the space charge distribution at different application times (10 s, 60 s, 300 s, 900 s, and 1800 s) was extracted, respectively.

3. Results

3.1. SEM. Scanning electron microscope (SEM) was used to observe TiO_2 nanoparticle dispersion and cross-sectional microstructure in XLPE. The SEM images of UN-TiO_2/XLPE and MDOS-TiO_2/XLPE (1 wt% and 5 wt%) are shown in Figure 4. It can be seen that TiO_2 nanoparticle dispersion was uniform in UN-TiO_2/XLPE nanocomposite, but agglomeration phenomenon was serious, with particle radius of 400~600 nm. However, the agglomeration phenomenon in MDOS-TiO_2/XLPE was better than UN-TiO_2/XLPE nanocomposite, with particle radius of 25~200 nm. Therefore, the TiO_2 nanoparticle dispersion and compatibility in XLPE could be improved to a certain extent by MDOS coupling agent. Relevant researches showed that hydroxyl groups on the UN-TiO_2 nanoparticles surface could easily react with each other to form a chemical bond, leading to the TiO_2 nanoparticles' tendency to agglomerate. For the MDOS-TiO_2 nanoparticles, however, fewer hydroxyl groups were on TiO_2 nanoparticles surface, because the hydroxyl groups were replaced by the functional groups of MDOS, which had difficulty forming a chemical bond with hydroxyl groups. Thus, the interaction between TiO_2 nanoparticles was weakened, and the dispersion of TiO_2 nanoparticles in XLPE was improved [18].

3.2. Volume Resistivity. The volume resistivity of Pure-XLPE and TiO_2/XLPE nanocomposite is shown in Figure 5. The volume resistivity of both UN-TiO_2/XLPE and MDOS-TiO_2/XLPE was larger than of Pure-XLPE, and it increased with the increase of filling concentration; MDOS-TiO_2/XLPE nanocomposite had the largest volume resistivity at different concentration points, but all of the values were in the same order of magnitude. Relevant researches showed that more charges are trapped in the TiO_2/XLPE nanocomposite, which could capture carriers and impede the movement of carriers, improving the volume resistivity of TiO_2/XLPE nanocomposites [19].

3.3. Space Charge Distribution. Figure 6 shows the space charge distribution of Pure-XLPE. A large number of heterocharges accumulated at XLPE-electrode interface; that is to say, negative charges accumulated near the anode and positive charges accumulated near the cathode. In addition, two charge peaks appeared in the middle of the sample. The positive charge peak A was near the anode, the negative charge peak B was near the cathode, and the peak charge volume increased with time.

Figures 7(a)~7(c) show the space charge distribution of UN-TiO_2/XLPE with different filling concentrations. The heterocharge near XLPE/electrode interface mostly disappeared and some stable negative charges accumulated inside the samples. In addition, the quantity of negative charges in the sample was maximum, when the filling concentration was 1 wt%.

Figures 8(a)~8(c) show the space charge distribution of MDOS-TiO_2/XLPE with different filling concentrations. Similarly, the heterocharge near XLPE-electrode interface mostly disappeared and some stable negative charges accumulated in the middle of the MDOS-TiO_2/XLPE samples. However, homocharge injection was more obvious, especially positive charge injection near the anode, and homocharge injection volume decreased with the increase of filling concentration.

The electric field distribution of Pure-XLPE and TiO_2/XLPE under DC stress of −30 kV/mm at 1800 s is shown in Figure 9. The electric field distortion at the electrode was obvious in Pure-XLPE, because a large number of heterocharges accumulated at XLPE-electrode interface, and the maximum electric field near the anode was −36 kV/mm. The electric field distribution was improved obviously in nanocomposites, and the weakest electric field distortion in MDOS-TiO_2/XLPE nanocomposites was observed. In particular, the internal electric field strength of MDOS-TiO_2/XLPE was basically the same as the external electric field.

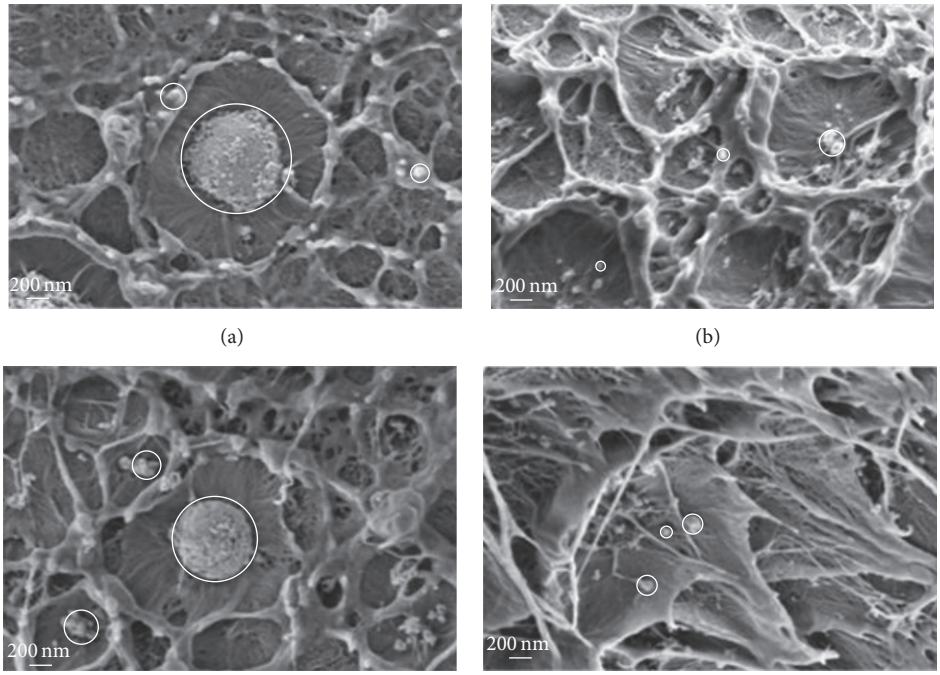

Figure 4: SEM of TiO_2/XLPE. (a) UN-TiO_2/XLPE (1 wt%), (b) MDOS-TiO_2/XLPE (1 wt%), (c) UN-TiO_2/XLPE (5 wt%), and (d) MDOS-TiO_2/XLPE (5 wt%).

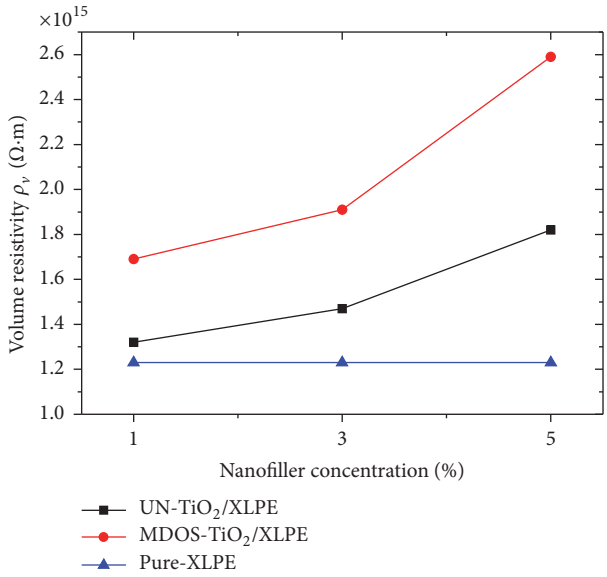

Figure 5: Volume resistivity of Pure-XLPE and TiO_2/XLPE.

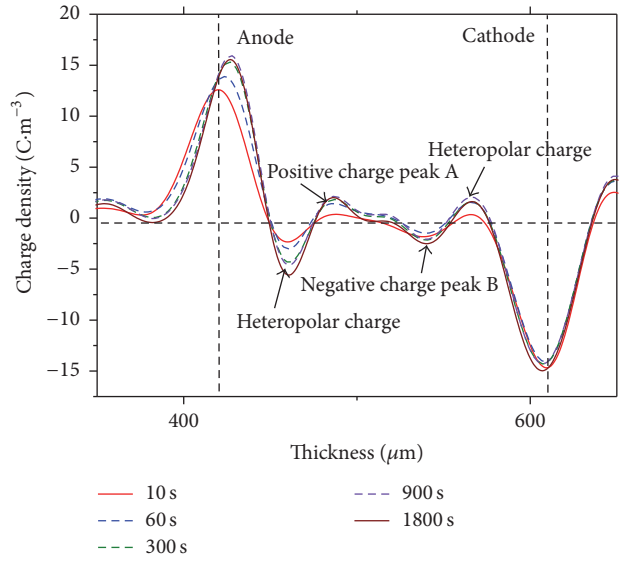

Figure 6: Space charge distribution of Pure-XLPE.

In order to further investigate the space charge characteristics of modified material, the mean volume density of space charge was used to quantitatively describe the space charge accumulation into TiO_2/XLPE, which can be calculated based on the charge density distribution, as shown in the following formula:

$$q\left(t; E_p\right) = \frac{1}{x_1 - x_0} \int_{x_0}^{x_1} \left| q_P\left(x, t; E_p\right) \right| dx, \quad (1)$$

where x_0 and x_1 refer to the position of lower electrode and upper electrode, respectively (inductive charges at the sample-electrode interface were ignored), t refers to the polarization time, E_p refers to the polarized electric field, and $q_P(x, t; E_p)$ refers to the charge density, and the absolute value was used in this paper.

Figure 10 shows the relationship between mean volume density of space charge and polarization time. It could be seen

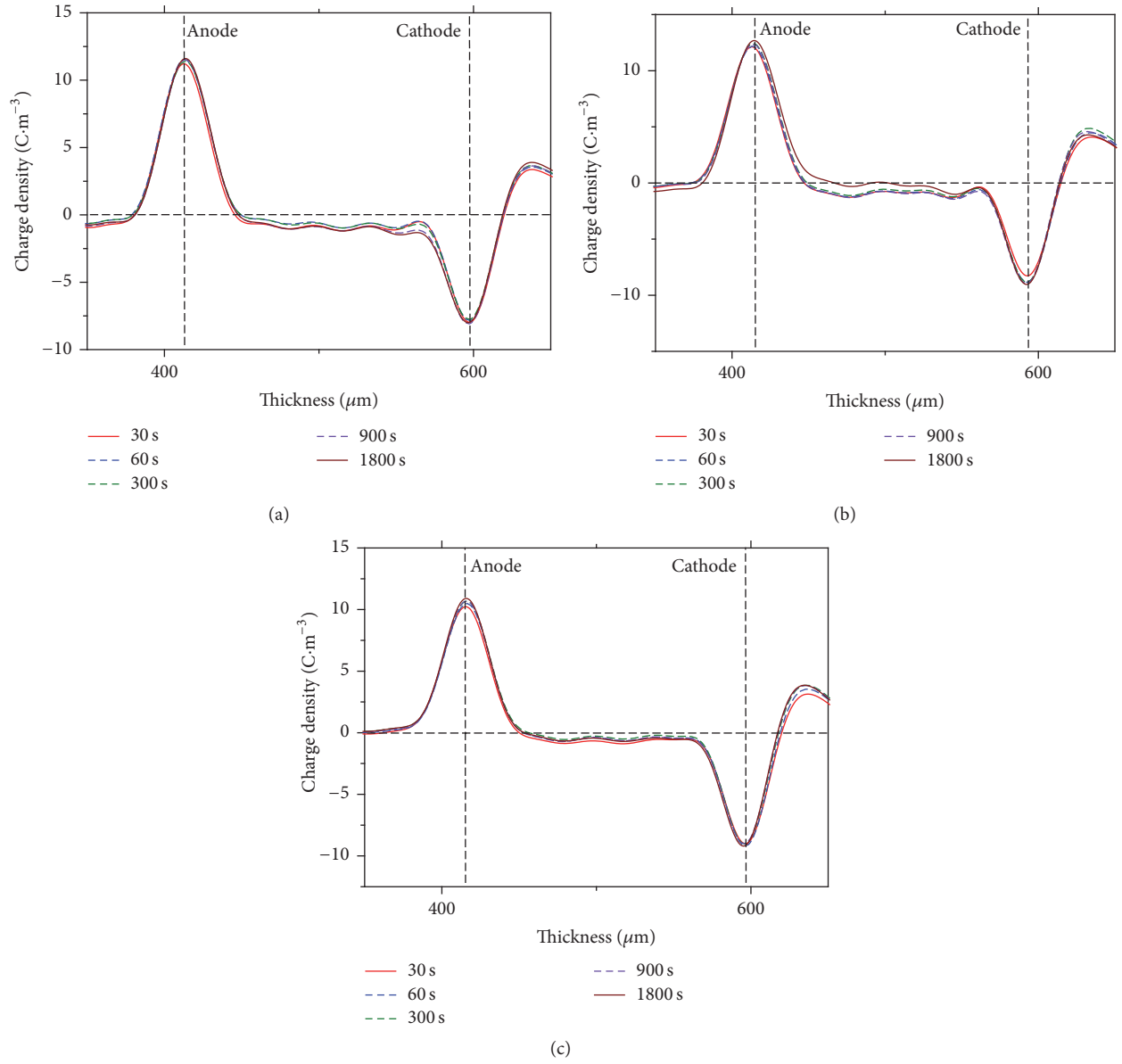

Figure 7: Space charge distribution of UN-TiO_2/XLPE with different concentrations at different times. (a) 1 wt%, (b) 3 wt%, and (c) 5 wt%.

that Pure-XLPE had the largest charge accumulation volume, with the volume density of space charge of 1.85 C/m^3. However, the volume density of space charge for UN-TiO_2/XLPE nanocomposite ranged from 0.85 C/m^3 to 1.27 C/m^3, while that for MDOS-TiO_2/XLPE ranged from 0.60 C/m^3 to 0.76 C/m^3. No matter UN-TiO_2/XLPE or MDOS-TiO_2/XLPE nanocomposite, the total charge accumulation volume has been well suppressed. Moreover, the MDOS-TiO_2/XLPE had less charge accumulation volume than UN-TiO_2/XLPE nanocomposite. In addition, the relationship between mean volume density of space charge and TiO_2 filling concentration was not obvious, but it could be seen from the overall trend that the space charge accumulation volume decreased with the increase of filling concentration.

4. Discussion

After the Pure-XLPE sample was polarized under −30 kV/mm DC voltage within 30 min, apparent heterocharge accumulated at XLPE-electrode interface and two charge peaks appeared in the middle of the sample, which was consistent with the results reported in the related literature [20, 21]. This phenomenon would be explained from two aspects in this paper. First, Montanari et al. measured the space charge of LDPE, XLPE, and other polymers under low electric field strength (such as 20 kV/mm), and it was found that space charge packets named "solitary waves" existed in polymers [21, 22]. The electronic "solitary waves" injected from the cathode and hole "solitary waves" injected from the anode were transferred to the opposite electrode under applied

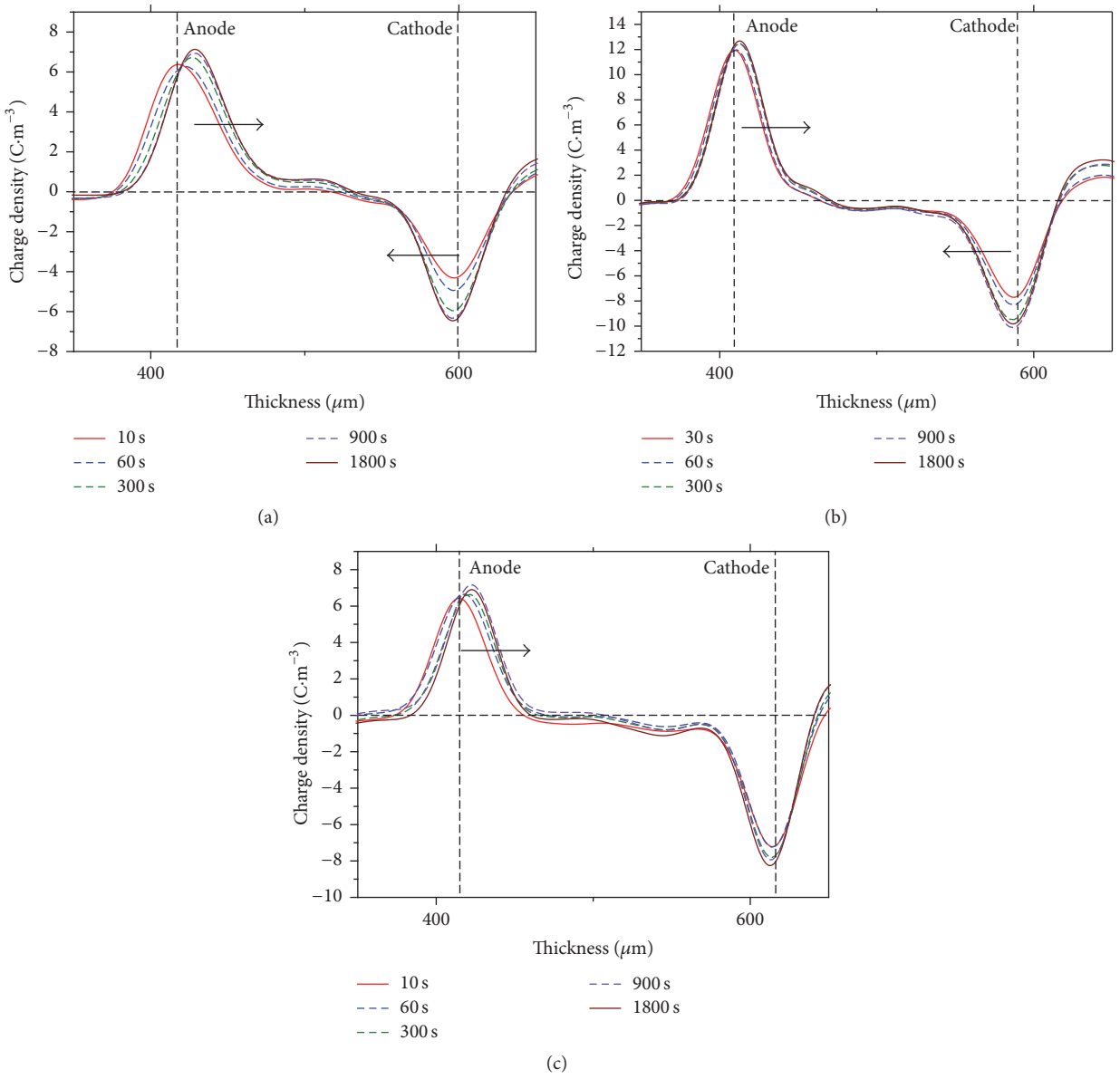

FIGURE 8: Space charge distribution of MDOS-TiO_2/XLPE with different concentrations at different times. (a) 1 wt%, (b) 3 wt%, and (c) 5 wt%.

electric field. The quantity of charge that flowed into the electrodes was less than that of accumulated charge due to "solitary waves" near electrodes, because there existed a potential barrier between XLPE and electrode interface. Then, a few heterocharges accumulated at XLPE-electrode interface, as shown in Figure 11.

Second, the impurities in XLPE medium (cross-linking agents, coupling agents, cross-linked products, and so on) were dissociated into positive and negative ions; the positive ions were transferred to the cathode and the negative ions were transferred to the anode under high electric field. According to the fast PEA testing, it was indicated that the "solitary waves" reached the opposite electrodes and established the equilibrium state, the process of which took several μm [22]. However, the migration rate of positive and negative ions was much slower compared to electrons and holes because of larger mass fraction and a large number of localized state restrictions in XLPE, causing the positive and negative ions to be easily captured by traps and to escape from traps difficultly [23]. Therefore, positive charge peak A and negative charge peak B appeared in the middle of the XLPE medium, as shown in Figure 11. In addition, the charge accumulation volume measured by PEA is net charge volume, which is the sum of electrons, holes, and positive and negative ions.

The heterocharge and total space charge accumulation were both suppressed in XLPE medium, when XLPE was filled with UN-TiO_2 and MDOS-TiO_2 nanoparticles. For the inhibition mechanism of space charge in nanocomposite media, Tanaka et al. considered that the diffuse layer of

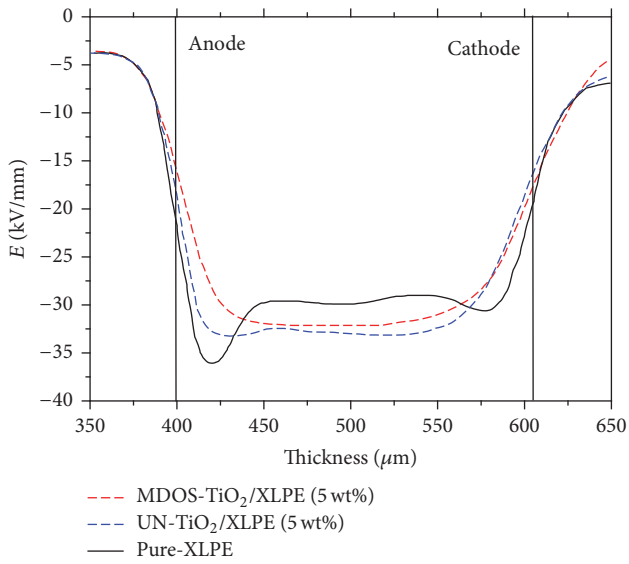

Figure 9: Electric field distribution of Pure-XLPE and TiO_2/XLPE under DC stress of −30 kV/mm at 1800 s.

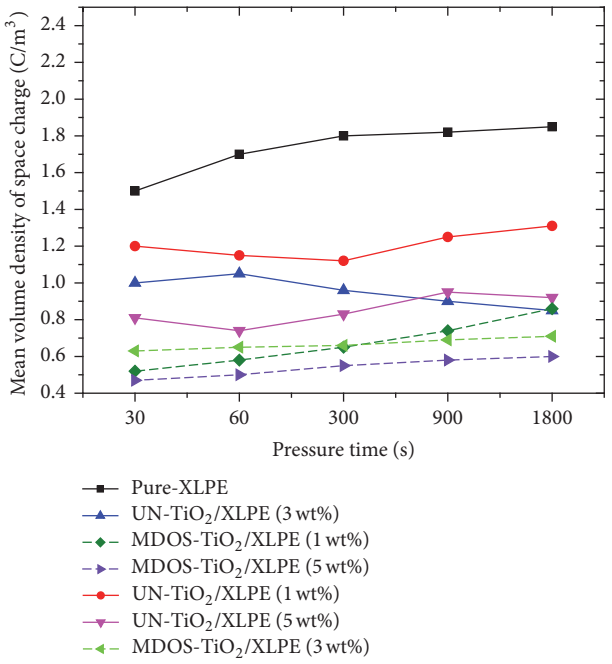

Figure 10: Mean volume density of space charge in samples.

XLPE-TiO_2 interface accumulated negative charges due to producing negative charges in polyethylene by friction. The diffuse layer attracts holes and rejects electrons, improving the potential barrier of electrons injection and reducing the potential barrier of holes injection [15]. This theory can be used to explain the enhancement of holes injection, but the inhibition of both electrons and holes injection and the disappearance of heterocharge cannot be reasonably explained. Another possibility was that the electrical conductivity of polyethylene was improved by filling nanoparticles, causing the injected charge to be quickly excreted from the matrix, so

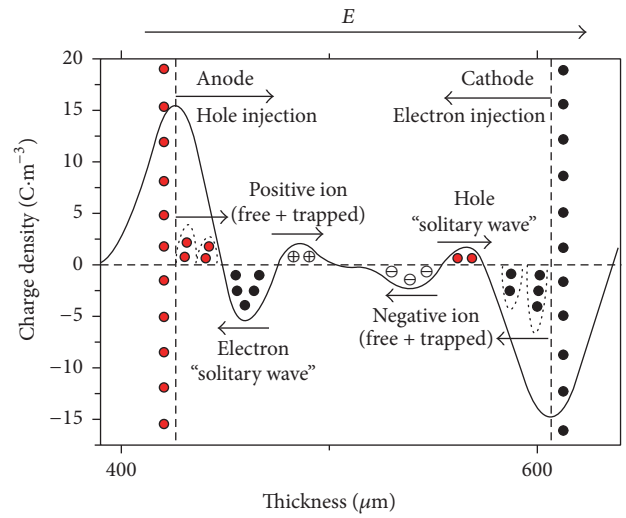

Figure 11: Schematic diagram of space charge accumulation in Pure-XLPE.

it was difficult to accumulate space charge [24]. However, the TiO_2/XLPE had larger volume resistivity and lower carrier mobility rate than Pure-XLPE (as shown in Figure 5), so the second explanation mechanism was not established.

In this paper, the inhibition of space charge and the disappearance of heterocharge were analyzed through trap characteristics. Figure 12 illustrates the carrier transport and interface electric field model based on trap characteristics, and E, E_1, and E_2 are the applied electric field, interface reverse electric field near the anode, and interface reverse electric field near the cathode, respectively. This model indicates that heterogeneous nucleation and steric hindrance in TiO_2/XLPE nanocomposite have a significant influence on crystallization process and changed the microcrystalline morphology of XLPE, producing a large number of uniform small spherocrystals and more interfaces between crystalline and amorphous regions [25]. These interfaces had lots of charge traps, which shortened the effective distance of "solitary waves" migration and greatly reduced carrier mobility. Therefore, few charges could reach the opposite electrodes and few space charges were accumulated to form heterocharge. In addition, the ionization process and neutralization process existed simultaneously, and low carrier mobility also enhanced the neutralization process between positive and negative charges and weakened the impurity ionization. So, the heterocharge disappeared in TiO_2/XLPE nanocomposite.

On the other hand, a large number of charges would be fixed in the vicinity of electrode interface because of the many traps in TiO_2/XLPE nanocomposite, leading to the accumulation of homocharge and the increase of interface reverse electric field (as shown in Figure 12, $E_1' > E_1$ and $E_2' > E_2$). So, the interface electric field decreased greatly, and the charges could not be easily injected into the matrix. Furthermore, the larger the trap density was, the lower the interface electric field was. For further explanation for TiO_2-XLPE interface, taking cathode electron injection

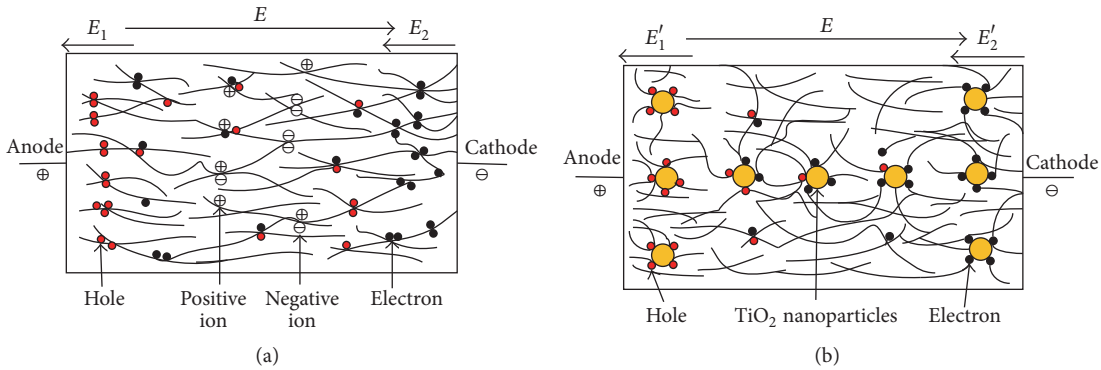

Figure 12: Carrier transport and interface electric field model based on trap characteristics. (a) Carrier transport in Pure-XLPE. (b) Carrier transport in TiO_2/XLPE.

as an example, an electron accumulation area is formed near the interface, and its width is shown in formula (2) [26]. It can be seen that the larger the trap density N_t, the narrower the width of the electron accumulation area and the larger the reverse electric field. Therefore, the higher the nanoparticles filling concentration, the more obvious the inhibition of charge injection from electrode and the fewer the space charges accumulated in the nanocomposite. At the same time, the accumulated homocharge strengthened the electric field in the middle of the matrix, so that the accumulated space charge could be timely transferred out of the material by volume conductivity. So, the space charge was suppressed obviously in TiO_2/XLPE nanocomposite.

$$\lambda = \frac{\pi}{2}\left(\frac{2kT\varepsilon_r\varepsilon_0}{e^2N_t}\right)^{1/2}\exp\left(\frac{\Psi_i - \chi - E_t}{2kT}\right), \quad (2)$$

where k refers to the Pohl Weitzman constant, T refers to the temperature, ε_0 refers to the vacuum dielectric constant, ε_r refers to the relative dielectric constant, e refers to the charge of the electron, N_t refers to the trap density, Ψ_i refers to the work function of the polymer, and χ refers to the electron affinity of the polymer.

According to the accumulated charge volume which is net charge volume, some stable negative charges accumulated in the middle of the TiO_2/XLPE nanocomposite; this is possibly because the electrons injected from the cathode were more than holes injected from the anode. The carriers were injected into polymer by hot electron emission under DC electric field, and the energy band diagrams for polymer-electrode system are shown in Figure 13, where Ψ_m is the work function of the electrode material, Ψ_i and χ are the same as those in formula (2), $\varphi = \Psi_m - \chi$ is charge injection barrier, E_c and E_v are the conduction band and valence band, E_g is band gap of polyethylene, E_{Fi} is Fermi energy level, and E is the applied electric field [27]. If there were no impurities in samples, the electrons from the electrode will skip over the electrode-XLPE interface through the Schottky effect and will be injected into the conduction band of XLPE. Electrons cannot easily transport through the conduction band, which easily fall into traps to form negative space charge because of conduction band bending near the interface (as shown in Figure 13(b)). Furthermore, the potential barrier of electrons injection is lower than that of holes injection, because of valence band bending near the interface (as shown in Figure 13(c)). In addition, the mass and volume of the electron are smaller than those of the hole, which also leads to a greater amount of injected electrons. Therefore, the injected electrons quantity was more than the injected holes quantity and, on the macroscopic level, some stable negative charges accumulated in the middle of the TiO_2/XLPE nanocomposite.

In particular, the homocharge injection was more obvious in MDOS-TiO_2/XLPE nanocomposite, and homocharge injection volume decreased with the increase of filling concentration. According to the potential well model proposed by Takada et al., deep traps would form at the interface between nanoparticles and polymer under applied electric field [16]. The TiO_2 nanoparticle dispersion was more uniform in MDOS-TiO_2/XLPE nanocomposite, according to the SEM images in Figure 4, generating larger TiO_2-XLPE interface area. So, the MDOS-TiO_2/XLPE has deeper traps than the UN-TiO_2/XLPE nanocomposite. These traps make a large number of charges injected from electrodes be fixed, forming homocharge near the electrodes. At the same time, there are more traps, and there are more homocharges. Therefore, the homocharge injection was more obvious in MDOS-TiO_2/XLPE nanocomposite. Nevertheless, the reverse electric field established by homocharge would also greatly reduce the interfacial electric field (as shown in Figure 12), which suppressed the electrons and holes injected from the electrodes, and the suppression effect was more obvious with increasing nanoparticle filling concentration. Consequently, the homocharge injection volume decreased with the increase of filling concentration, when the equilibrium state was reached again.

5. Conclusion

The work presented in this paper is concerned with the microstructure and space charge behaviors of Pure-XLPE and TiO_2/XLPE nanocomposite. Several significant findings were concluded.

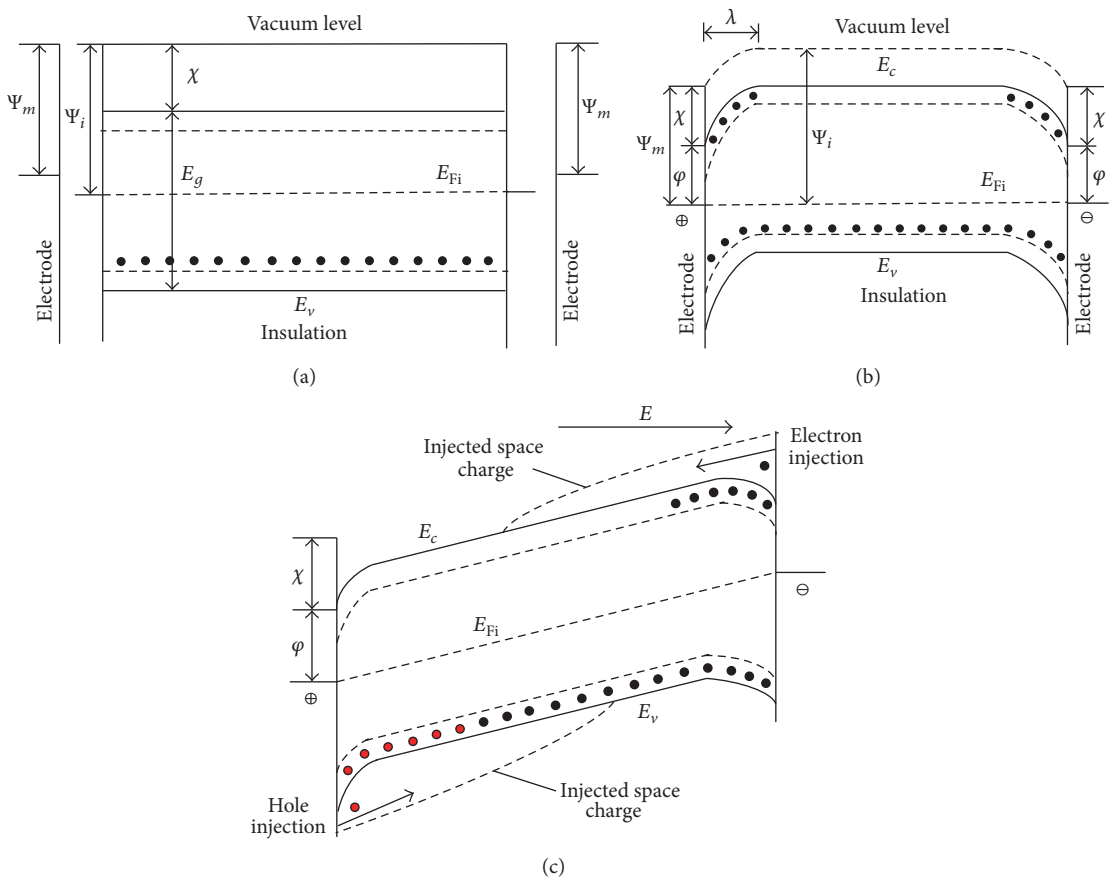

FIGURE 13: Energy band diagrams for polymer-electrode system. (a) No contact between sample and electrode, (b) contact between sample and electrode and no electric field, and (c) contact between sample and electrode and applied electric field.

(a) The TiO_2 nanoparticle agglomeration phenomenon in UN-TiO_2/XLPE nanocomposite is serious with the particle radius of 400~600 nm, but that of MDOS-TiO_2/XLPE is weak with the corresponding particle radius of 25~200 nm. It is concluded that MDOS coupling agent can improve TiO_2 nanoparticle dispersion and reduce the agglomeration of TiO_2 nanoparticles in XLPE matrix.

(b) The relationship of volume resistivity among the three kinds of samples in this paper is apparent, Pure-XLPE < UN-TiO_2/XLPE < MDOS-TiO_2/XLPE. The explanation is that TiO_2/XLPE nanocomposite has a large number of deep traps, which can reduce carrier mobility, improving the volume resistivity. In addition, the MDOS-TiO_2/XLPE nanocomposite has more traps than UN-TiO_2/XLPE, causing more carriers to be captured, and the MDOS-TiO_2/XLPE nanocomposite has the largest volume resistivity.

(c) The results of the PEA measurements show that TiO_2 nanoparticles have a significant influence on space charge accumulation behavior; the electric field distribution in TiO_2/XLPE is improved greatly under DC electric field. According to the analysis in this paper, on the one hand, a large number of interface regions generate lots of deep traps, which can shorten the effective distance of "solitary waves" migration and greatly reduce carrier mobility. On the other hand, low carrier mobility enhances the neutralization process and weakens the impurity ionization, leading to the disappearance of heterocharge in TiO_2/XLPE. The interface reverse electric field not only suppresses the charge injected from the electrodes, but also strengthens the electric field in the middle of the matrix, so that the accumulated space charge can be transferred out of the material timely.

(d) The homocharge injection is more obvious in MDOS-TiO_2/XLPE, and homocharge injection volume decreases with the increase of filling concentration. According to the analysis in this paper, the MDOS-TiO_2/XLPE nanocomposite has deeper traps than the UN-TiO_2/XLPE nanocomposite, causing more homocharges to be injected in the MDOS-TiO_2/XLPE. The reverse electric field established by homocharge is the main reason for the homocharge decrease with the increase of nanoparticles, increasing filling concentration.

Competing Interests

The authors declare that they have no financial or personal relationship with any people or any organization that may inappropriately influence their work and that there is no professional or commercial interest of any kind in all of the commercial entities mentioned in their paper.

Acknowledgments

The reported research was performed with funding from the National Key Basic Research Program of China (973 Program), Contract Grant no. 2015CB251003.

References

[1] B. Dang, J. He, J. Hu, and Y. Zhou, "Tailored sPP/silica nanocomposite for ecofriendly insulation of extruded HVDC cable," *Journal of Nanomaterials*, vol. 2015, Article ID 686248, 9 pages, 2015.

[2] H. Zheng, "Space charge monitoring in cables at low DC electrical field," in *Proceedings of the IEEE Conference on Electrical Insulation and Dielectric Phenomena (CEIDP '15)*, Ann Arbor, Miss, USA, October 2015.

[3] W. L. Zhang, Y. Dai, H. Zhao, and L. Zhong, "Influence of nanocomposites of LDPE doped with nano-MgO by different preparing methods on its dielectric properties," *Journal of Nanomaterials*, vol. 2015, Article ID 146260, 6 pages, 2015.

[4] Y. J. Lin, W. Du, D. Tu, W. Zhong, and Q. Du, "Space charge distribution and crystalline structure in low density polyethylene (LDPE) blended with high density polyethylene (HDPE)," *Polymer International*, vol. 54, no. 2, pp. 465–470, 2005.

[5] R. Liao, G. Bai, L. Yang, H. Cheng, Y. Yuan, and J. Guan, "Improved electric strength and space charge characterization in LDPE composites with montmorillonite fillers," *Journal of Nanomaterials*, vol. 2013, Article ID 712543, 7 pages, 2013.

[6] B. Ouyang, J. Zhao, Z. Chen, W. Li, J. Li, and X. Wang, "Influence of aging mode on space charge distribution of AC XLPE cables," *High Voltage Engineering*, vol. 38, no. 8, pp. 2123–2128, 2012.

[7] W. U. Jiandong, Y. Yin, L. Lan, Q. Wang, L. I. Xuguang, and D. Xiao, "The influence of nano-filler concentration on space charge behavior in LDPE/Silica nanocompo-site," *Proceedings of the CSEE*, vol. 32, no. 28, pp. 177–183, 2012.

[8] J. M. Yang, C. Liu, C. Zheng, H. Zhao, X. Wang, and M. Gao, "Effects of interfacial charge on the DC dielectric properties of nanocomposites," *Journal of Nanomaterials*, vol. 2016, Article ID 2935202, 11 pages, 2016.

[9] Y. Yin, J. Chen, Z. Li, and D. Xiao, "High field conduction of the composites of low-density polyethylene/nano-SiO_2," *Transactions of China Electrotechnical Society*, vol. 21, no. 2, pp. 22–26, 2006.

[10] J. Chen, Y. Yin, Z. Li, D. M. Xiao, and Z. M. Dang, "The effect of electrically pre-stressing of high field conduction in the nanocomposite of polyethylene and nano-SiO_2," *Proceedings of the CSEE*, vol. 26, no. 7, pp. 146–151, 2006.

[11] P. Yan, Y. Zhou, G. Sun, and N. Yoshimura, "Influence of morphology and thermal stability on tree initiation in polyethylene films," in *Proceedings of the IEEE Annual Report Conference on Electrical Insulation and Dielectric Phenomena*, pp. 249–252, Kitchener, Canada, October 2001.

[12] Z. Ma, X. Huang, P. Jiang, and G. Wang, "Effect of silane-grafting on water tree resistance of XLPE cable insulation," *Journal of Applied Polymer Science*, vol. 115, no. 6, pp. 3168–3176, 2010.

[13] Y. Yamano and M. Ilzuka, "Role of additive for polycyclic compound in the suppression of electrical tree generation in LDPE," in *Proceedings of the IEEE International Symposium on Electrical Insulating Materials*, vol. 345, 1255903 pages, September 2008.

[14] T. J. Lewis, "Interfaces are the dominant feature of dielectrics at the nanometric level," *IEEE Transactions on Dielectrics and Electrical Insulation*, vol. 11, no. 5, pp. 739–753, 2004.

[15] T. Tanaka, M. Kozako, N. Fuse, and Y. Ohki, "Proposal of a multi-core model for polymer nanocomposite dielectrics," *IEEE Transactions on Dielectrics and Electrical Insulation*, vol. 12, no. 4, pp. 669–681, 2005.

[16] T. Takada, Y. Hayase, Y. Tanaka, and T. Okamoto, "Space charge trapping in electrical potential well caused by permanent and induced dipoles for LDPE/MgO nanocomposite," *IEEE Transactions on Dielectrics and Electrical Insulation*, vol. 15, no. 1, pp. 152–160, 2008.

[17] S. Kango, S. Kalia, A. Celli, J. Njuguna, Y. Habibi, and R. Kumar, "Surface modification of inorganic nanoparticles for development of organic-inorganic nanocomposites—a review," *Progress in Polymer Science*, vol. 38, no. 8, pp. 1232–1261, 2013.

[18] Y. Sun, Z. Zhang, and C. P. Wong, "Study on mono-dispersed nano-size silica by surface modification for underfill applications," *Journal of Colloid and Interface Science*, vol. 292, no. 2, pp. 436–444, 2005.

[19] K. Wu, X. Chen, X. Liu, X. Wang, Y. Cheng, and L. A. Dissado, "Study of the space charge behavior in polyethylene nanocomposites under temperature gradient," in *Proceedings of the 2011 International Conference on Electrical Insulating Materials (ISEIM '11)*, pp. 84–87, Kyoto, Japan, September 2011.

[20] G. Chen, T. Y. G. Tay, A. E. Davies, Y. Tanaka, and T. Takada, "Electrodes and charge injection in low-density polyethylene using the pulsed electroacoustic technique," *IEEE Transactions on Dielectrics and Electrical Insulation*, vol. 8, no. 6, pp. 867–873, 2001.

[21] G. C. Montanari, D. Fabiani, and L. A. Dissado, "A new conduction phenomenon observed in polyethylene and epoxy resin: ultra-fast soliton conduction," *Journal of Polymer Science Part B: Polymer Physics*, vol. 49, no. 16, pp. 1173–1182, 2011.

[22] J. Zhao, G. Chen, and P. L. Lewin, "Investigation into the formation of charge packets in polyethylene: experiment and simulation," *Journal of Applied Physics*, vol. 112, no. 3, Article ID 034116, 2012.

[23] Q. Zhong, L. Lan, J. Wu, and Y. Yin, "The influence of cross-linked by-products on space charge behaviour in XLPE," *Proceedings of the Chinese Society of Electrical Engineering*, vol. 35, no. 11, pp. 2903–2910, 2015.

[24] T. Tanaka, "Dielectric nanocomposites with insulating properties," *IEEE Transactions on Dielectrics and Electrical Insulation*, vol. 12, no. 5, pp. 914–928, 2005.

[25] F. Tian, Q. Lei, X. Wang, and Y. Wang, "Effect of deep trapping states on space charge suppression in polyethylene/ZnO nanocomposite," *Applied Physics Letters*, vol. 99, no. 14, Article ID 142903, 2011.

[26] Y. Sekii, "A study on the space charge formation in XLPE," in *Proceedings of the IEEE Conference on Electrical Insulation and Dielectric Phenomena*, pp. 327–332, Kitchener, Canada, October 2001.

[27] D.-M. Tu, X. Wang, Z.-P. Lü, K. Wu, and Z.-R. Peng, "Formation and inhibition mechanisms of space charges in direct current polyethylene insulation explained by energy band theory," *Acta Physica Sinica*, vol. 61, no. 1, pp. 17–24, 2012.